Developmental Biology 427 (2017) 219–229

Contents lists available at ScienceDirect

Developmental Biology

journal homepage: www.elsevier.com/locate/developmentalbiology

Review article

The origin and diversification of the developmental mechanisms that pattern the vertebrate head skeleton

Tyler Square[a,*], David Jandzik[a,b,c], Marek Romášek[a,c], Robert Cerny[c], Daniel Meulemans Medeiros[a,*]

[a] Department of Ecology and Evolutionary Biology, University of Colorado, Boulder, CO 80309, USA
[b] Department of Zoology, Comenius University in Bratislava, Bratislava 84215, Slovakia
[c] Department of Zoology, Charles University in Prague, 128 44 Prague, Czech Republic

ABSTRACT

The apparent evolvability of the vertebrate head skeleton has allowed a diverse array of shapes, sizes, and compositions of the head in order to better adapt species to their environments. This encompasses feeding, breathing, sensing, and communicating: the head skeleton somehow participated in the evolution of all these critical processes for the last 500 million years. Through evolution, present head diversity was made possible via developmental modifications to the first head skeletal genetic program. Understanding the development of the vertebrate common ancestor's head skeleton is thus an important step in identifying how different lineages have respectively achieved their many innovations in the head. To this end, cyclostomes (jawless vertebrates) are extremely useful, having diverged from jawed vertebrates approximately 400 million years ago, at the deepest node within living vertebrates. From this ancestral vantage point (that is, the node connecting cyclostomes and gnathostomes) we can best identify the earliest major differences in development between vertebrate classes, and start to address how these might translate onto morphology. In this review we survey what is currently known about the cell biology and gene expression during head development in modern vertebrates, allowing us to better characterize the developmental genetics driving head skeleton formation in the most recent common ancestor of all living vertebrates. By pairing this vertebrate composite with information from fossil chordates, we can also deduce how gene regulatory modules might have been arranged in the ancestral vertebrate head. Together, we can immediately begin to understand which aspects of head skeletal development are the most conserved, and which are divergent, informing us as to when the first differences appear during development, and thus which pathways or cell types might be involved in generating lineage specific shape and structure.

1. Introduction

Vertebrates emerged during the Cambrian explosion more than 500 million years ago. They have since attained an incredible degree of specialization and morphological diversity, which likely played a role in their becoming the most species-rich and geographically dispersed deuterostomes on the planet. This success is thought to have been made possible, in large part, by the origin and elaboration of the vertebrate head skeleton. In the earliest vertebrates, the facilitation of pharyngeal pumping by the head skeleton seems most probably to be a major source of early vertebrate success, by simply increasing the rates of respiration and filter feeding (Gans and Northcutt, 1983; Northcutt and Gans, 1983). While many modern vertebrates (namely tetrapods) have discarded this pharyngeal pumping strategy in their adult forms, the head skeleton still performs many basic functions in all vertebrates by supporting and protecting the brain and anterior sense organs. Aside from its ancestral and shared functions, the head skeleton is also extraordinarily evolvable, having proven itself capable of taking on a wide array of adaptive shapes and compositions for respiration, feeding, communication, and sensing the environment. The fossil record suggests this flexibility arose very early in the vertebrate lineage, with an impressive diversity of both jawless and jawed forms arising within 100 million years after the first vertebrates appeared (Fig. 1).

Though the fossil record shows when the adult head skeleton arose and how it has diversified, it tells us nothing about the developmental and genetic bases of its extreme evolvability or its origin. The modern comparative or “evolutionary developmental” approach allows us to deduce conserved and divergent features of development, and functionally link these to similarities and differences in adult morphology. In this review we examine what is known about early head skeleton

* Corresponding authors.
E-mail addresses: square@colorado.edu (T. Square), daniel.medeiros@colorado.edu (D.M. Medeiros).

http://dx.doi.org/10.1016/j.ydbio.2016.11.014
Received 2 August 2016; Received in revised form 6 October 2016; Accepted 20 November 2016
Available online 21 November 2016

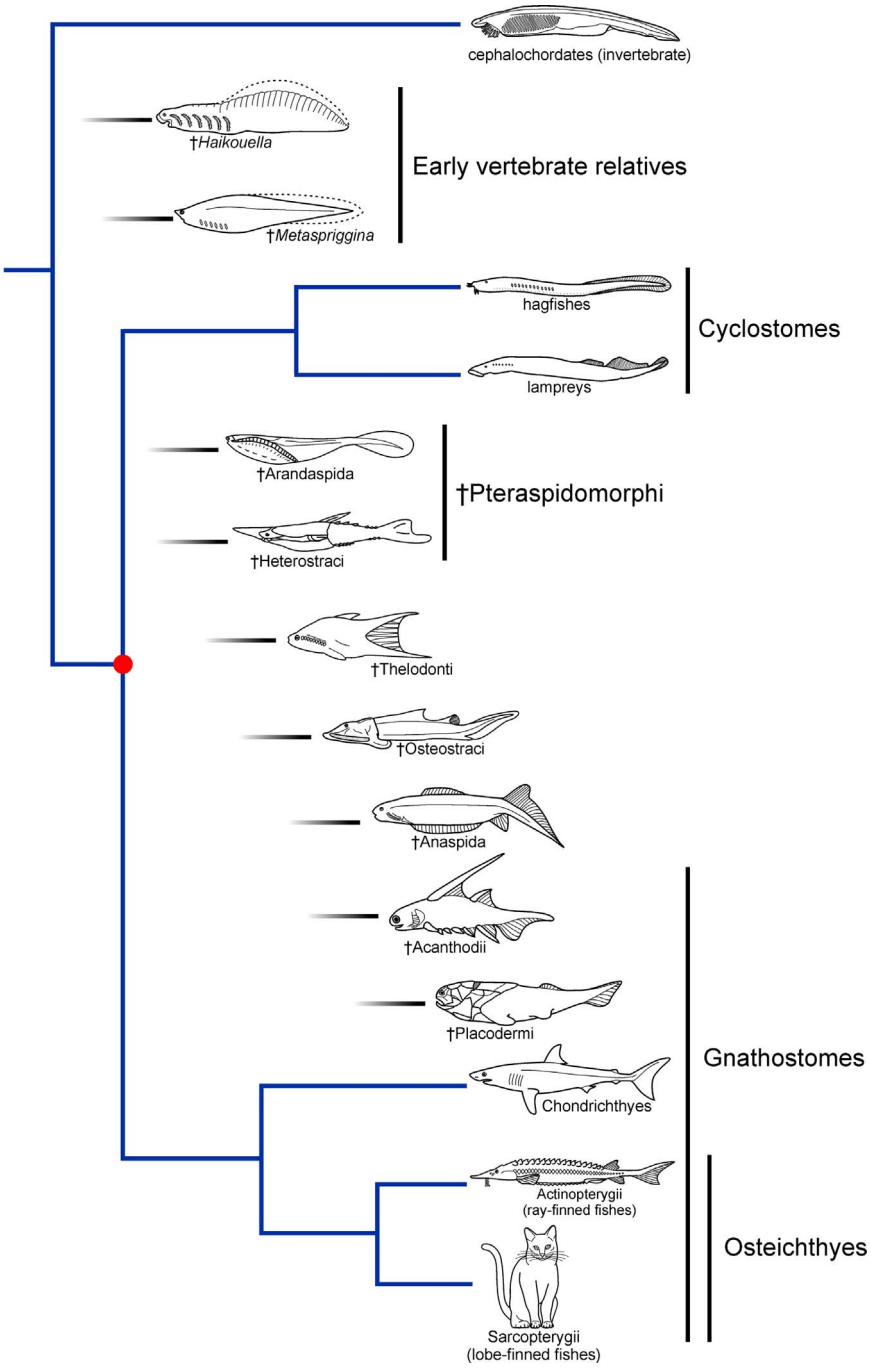

Fig. 1. A cladogram of major vertebrate groups. Extinct groups are indicated with a (†). Relatedness of only the extant groups is depicted with blue lines. The node representing the position of the last common ancestor to all living vertebrates is indicated with a red circle. The position along the X-axis for each fossil group's branch shows their relative approximate time of presence in the fossil record. The length of every line is the same for these extinct groups, and is not representative of the known duration of each group's history on earth (which is extremely variable considering these groups). Some of these groups may be paraphyletic. Some groups are very diverse; only a single living member or well-characterized fossil from each group is pictured. Some major groups not shown include Conodonta and Galeapsida. Some illustrations are after those within Hildebrand and Goslow (2001) and Janvier (1996).

development in a broad sampling of living vertebrates, including the only living jawless vertebrates, the cyclostomes. The cyclostomes consist of two groups: hagfishes and lampreys. Historically, there has been some debate about whether cyclostomes are monophyletic or paraphyletic, however various sequence-based analyses support the former scenario (Delarbre et al., 2002; Heimberg et al., 2010; Stock and Whitt, 1992). The fossil record reveals that cyclostomes represent only a fraction of agnathan (jawless vertebrate) diversity (see Fig. 1) and suggests that modern adult lampreys and hagfishes possess highly derived skeletal morphologies and lifestyles, a phenomenon that is also easily observed in many gnathostome (jawed vertebrate) groups (e.g. the evolution of the middle ear bones from pharyngeal arch structures in mammals). Nevertheless, modern cyclostomes offer our only window into agnathan developmental genetics. Furthermore, larval lampreys possess a simple head skeleton composed mainly of cartilaginous PAs, and appear grossly similar in morphology to the earliest fossil agnathans. Thus larval lampreys likely retain many ancestral features lost or masked in gnathostomes.

In this phylogenetic context, here we use comparisons of cyclostome and gnathostome head skeleton development in combination with the fossil record to support several key conclusions about the head skeleton of the most recent common ancestor of modern vertebrates,

found at the node bearing the red circle in Fig. 1: 1) it formed mainly from a set of three distinct streams of cranial neural crest cells (CNCCs), 2) after migration into the pharynx, these cells activated a 'cartilage gene regulatory network (GRN)' of at least three genes, as well as a combinatorial code of at least 10 transcription factors in particular oropharyngeal subdomains, and 3) these subpopulations of skeletal precursors differentiated into an endoskeleton consisting mainly of pharyngeal arches (PAs), throughout which histologically distinct cartilage types were deployed. Taken together, the conserved aspects of head skeleton formation and patterning suggest that major differences in head skeleton morphology are likely due to changes in differentiation and morphogenetic programs downstream of a conserved developmental prepattern. However, some striking differences in this prepattern are evident, and may be tied to some specific large-scale differences in morphology between modern agnathans and gnathostomes, and also between gnathostome groups.

2. Modern vertebrate head skeletons are derived from CNCCs that migrate as three streams

In both modern cyclostomes and gnathostomes, vital dye labeling and gene expression suggest all cartilaginous PA and pre-oral skeletal elements are derived mainly from CNCCs (Kuratani et al., 2016; McCauley and Bronner-Fraser, 2003; Noden, 1978; Santagati and Rijli, 2003). After being specified by highly conserved gene regulatory interactions (Sauka-Spengler et al., 2007; Simoes-Costa and Bronner, 2015), CNCCs migrate ventrally from the neural border during and after neurulation, populating the pharynx and oral region. In both gnathostomes and lampreys, CNCCs are specified at all positions along the neural plate border from the midbrain through the hindbrain, but congregate into three main streaming populations as they proceed towards the pharynx: pre-oral and PA1 cells in the 1st stream, PA2 cells in the 2nd stream, and branchial arch (PAs 3+) cells in the 3rd stream (Fig. 2; reviewed by Theveneau and Mayor (2012)). The CNCC-negative regions (between the streams) are consistently situated beneath rhombomeres 3 and 5 of the brain in both lampreys and gnathostomes (Minoux and Rijli, 2010). These spatial similarities mark high conservation of this general migratory architecture.

While CNCC migration patterns are generally conserved across vertebrates, there are some notable differences between the lamprey and gnathostome 3rd CNCC streams. In gnathostomes the 3rd stream originates from rhombomeres 5–7, and becomes progressively subdivided as it is still migrating and after migration (Minoux and Rijli, 2010). By contrast, the 3rd 'stream' of CNCCs in lamprey behaves more like a sheet, and emerges from a broad domain that includes 5–7th rhombomeres (Kuratani et al., 1998a) and part of the presumptive spinal cord, a region that would give rise to trunk neural crest in gnathostomes (Fig. 2). The reason for this is unclear, though it may simply reflect the fact that lamprey has a relatively long pharynx consisting of seven branchial arches (PA3-PA9). Nevertheless, in both lineages, the branchial arch neural crest cells become segregated in concert with pharyngeal pouch morphogenesis, and end up as separated 'tubes' of ectomesenchyme surrounding a mesodermal core (Cerny et al., 2004), flanking each gill slit.

Notably, the posterior PAs (the branchial arches) tend to be more homogenous both within and among species with regard to their gene expression patterns and eventual morphology. This contrasts with PA1 and PA2, which each come from unique streams of CNCCs; these are far more specialized in their gene expression and eventual morphology both within a given vertebrate's PAs, and among vertebrates. How and when separate 1st, 2nd, and 3rd streams evolved, and began to give rise to morphologically distinct derivatives is unclear. However, it is possible that the first CNCC to migrate from the neural tube was already divided into molecularly distinct anteroposterior populations by hox gene expression carried over from the CNS. Physical segregation of 3rd stream CNCCs from each other may evolved later in concert with

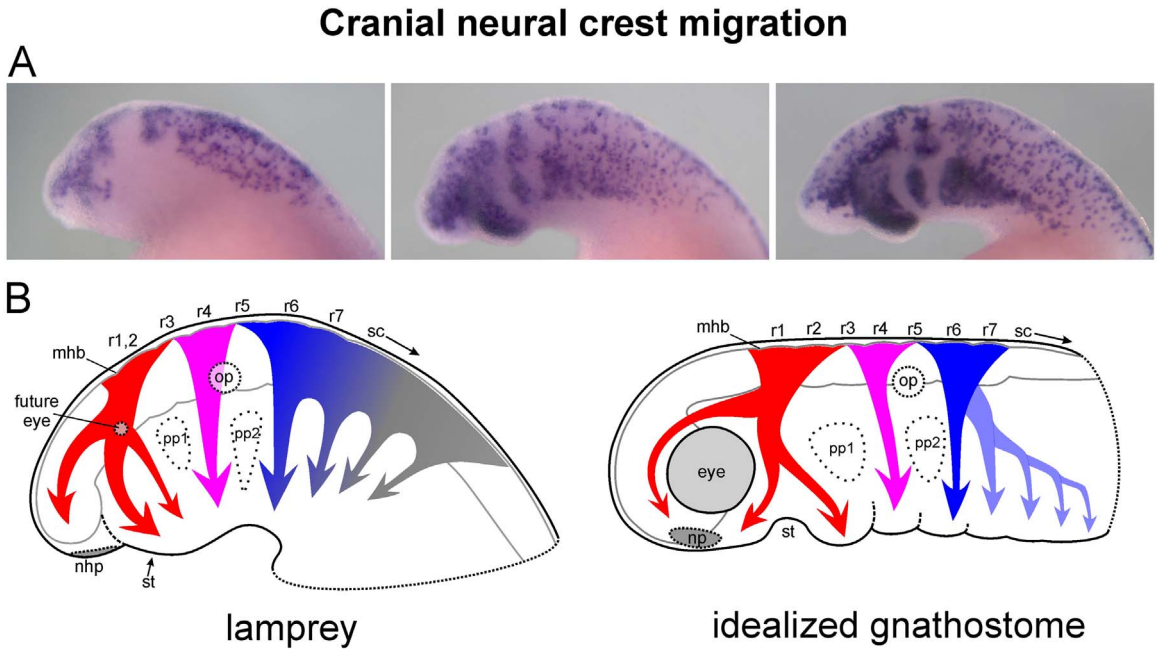

Fig. 2. Vertebrate cranial neural crest migration occurs as three topographically conserved streams. (A) Left lateral views of early pharyngula stage lamprey embryos (*Petromyzon marinus;* Tahara stage 21–23 (Tahara, 1988)) stained via *in situ* hybridization for *ednrb* transcripts (see Square et al., 2016 for a broader staging series of *ednrb in situ* hybridizations). This gene marks migratory skeletogenic cranial neural crest, among other neural crest derivatives. (B) A cartoon of early cranial neural crest migration in lamprey and an idealized gnathostome. The three homologous populations of CNCCs are indicated by different colors (red, pink, and blue); the sub-arrows within each of these streams are meant to depict general directions of cell migration, but do not explicitly indicate stream subdivisions. Each uniquely colored stream is molecularly defined by *hox* expression (see text). The 3rd stream in lamprey appears to have some contribution from the trunk (sc, spinal cord; see text); this is partially colored gray. The posteriormost arches of the gnathostome are slightly transparent to indicate that these splitting events occur after the population of cells is already moving ventrally (a process coincident with pharyngeal pouch formation [see text]). An outline of the brain is shown in gray. mhb, midbrain/hindbrain boundary; nhp, nasohypophyseal plate; np, nasal placode; op, otic placode; pp1 and pp2, pharyngeal pouches 1 and 2; r1-7, rhombomeres 1–7; sc, spinal cord; st, stomodeum.

the otic capsule, which is a conserved landmark for the boundary between the 2nd versus 3rd streams in all vertebrates.

When the three streams began giving rise to morphologically distinct derivatives is even more speculative, as all extant vertebrates display highly specialized PA1 and PA2 and posterior PA morphologies. Looking to the fossil record, some extinct vertebrate relatives also possess specialized cartilages around the mouth, as does the invertebrate amphioxus (Jandzik et al., 2015), but the developmental origin of these fossil structures (specifically whether they are PA-derived or not) is extremely difficult to assess. Irrespective of the timing of PA1 and PA2 specialization, gene expression (see below) and their resemblance to the PAs of fossil chordates indicates that PAs derived from the 3rd stream are likely the least developmentally derived, and might offer the best possible reconstruction of ancestral PA patterning at their first appearance in the vertebrate stem (discussed below).

3. Transcription factor expression in the vertebrate head skeleton

3.1. A conserved cellular environment, a conserved cartilage GRN, and a conserved tissue type

In both cyclostomes and gnathostomes, CNCCs entering the pharynx and oral region are exposed to a range of intercellular signals that regulate proliferation, differentiation, and morphogenesis. These include bone morphogenetic proteins (BMPs), Fibroblast growth factors (FGFs), Endothelins (Edns), retinoic acid (RA), and Hedgehog (Hh) (reviewed by Santagati and Rijli (2003)). In lamprey, the expression of key pathway members has been documented in and/or surrounding the pre-skeletal CNCCs for each of these signal types (Campo-Paysaa et al., 2015; Jandzik et al., 2014; Kuraku et al., 2010; McCauley and Bronner-Fraser, 2004; Medeiros and Crump, 2012; Sugahara et al., 2011; Square et al., 2016). Furthermore, the function of FGF and RA signaling has been addressed in lamprey, and found to be generally conserved with gnathostomes (Jandzik et al., 2014; Kuratani et al., 1998b). In addition to entering a similar intercellular signaling environment, CNCCs of both lampreys and gnathostomes differentiate into collagen-containing cellular cartilage and related skeletal tissues, such as joint tissue (gnathostomes) and soft mucocartilage (lamprey) (Cattell et al., 2011; Crump et al., 2004; Medeiros and Crump, 2012; Zhang et al., 2006). Consistent with this, gnathostome and lamprey CNCCs activate the same core set of chondrogenic regulators, including SoxE, Twist, and Ets (Meulemans and Bronner-Fraser, 2004). These genes are activated in the developing amphioxus oral cirri skeleton (Jandzik et al., 2015), a non-vertebrate cartilage, and *soxE* genes are expressed in the cartilage of horseshoe crabs and cuttlefish (Tarazona et al., 2016). This indicates that a core cellular cartilage differentiation program was already present before vertebrates arose, with a rudimentary version of this gene regulatory cascade likely predating the protostome/deuterostome divergence.

3.2. Combinatorial expression of alx, hand, msx, and prrx, define spatially conserved precursor populations in the PAs of all vertebrates

In addition to a core set of transcription factors that appear to drive skeletal differentiation in all CNCCs, there are several others expressed only in subsets of head skeleton precursors in both cyclostomes and gnathostomes (Fig. 3). For simplicity, we use the combined expression of all known paralogs of a given gene group when defining which regions are positive for a gene type (e.g. an *msx* positive domain means there is at least one *msx* gene expressed there, but there could be multiple). Together, these genes appear to act combinatorially to confer 'module-specific' identity upon CNCC subpopulations. In gnathostomes, most of these genes are known to affect different regions of head skeleton development in unique ways, though more work is needed to understand precisely how these genes confer regional shape and morphology. The conserved expression of these factors in all modern vertebrates suggests they mark evolutionarily conserved subpopulations of skeletal precursors present in their most recent common ancestor. Although these developmental modules of CNCCs are likely deeply homologous, if not homologous *sensu stricto* (or 'historically' homologous), it is less clear if the adult skeletal structures derived from them can be considered homologous in either a deep or strict/historical sense (for a discussion of deep homology, see Shubin et al. (2009)).

The dorsal and ventral poles of all vertebrate PAs examined to date express a similar combination of transcription factors: *alx* (Beverdam and Meijlink, 2001; Cattell et al., 2011; Compagnucci et al., 2013; Dee et al., 2013; McGonnell et al., 2011; Square et al., 2015), *hand* (Cerny et al., 2010; Charite et al., 2001; Compagnucci et al., 2013; Firulli, 2003; Square et al., 2015), *msx* (Antonopoulou et al., 2004; Cerny et al., 2010; Compagnucci et al., 2013; Square et al., 2015; Swartz et al., 2011), and *prrx* (Compagnucci et al., 2013; Hernandez-Vega and Minguillon, 2011; Square et al., 2015; ten Berge et al., 1998) transcripts can be found in both lamprey and gnathostomes in broadly similar patterns (Fig. 3; Fig. S1). In the ventral PAs all four of these genes are transcribed, though in lamprey ventral *alx* expression is absent from PA1 and PA2 (Cattell et al., 2011). Skeletogenic mesenchyme in the dorsal PAs of catshark, *Xenopus,* and mouse also express *msx* and *prrx*, though this domain appears to be only *prrx* positive in at least zebrafish. The intermediate domain between the poles (the light blue '*dlx* only' module in Fig. 3) in all vertebrates is marked by the exclusion of these four polar PA gene transcripts, but this domain also consistently overlaps the region wherein the highest number of *dlx* genes are expressed (discussed below; Fig. 4). Combined, *alx, hand, msx*, and *prrx* represent an ancient PA polarity scheme that molecularly designates CNCCs to dorsalmost, intermediate, and ventralmost identities. The function of all four of these genes are shown in various gnathostome models (Antonopoulou et al., 2004; Beverdam et al., 2001; ten Berge et al., 1998; Yanagisawa et al., 2003), however functional data from any cyclostome is lacking.

3.3. Nested dlx expression marks dorsal, ventral and intermediate skeletal precursor populations in the PAs of all living vertebrates

In gnathostomes, the *dlx* genes form six main orthology groups (1–6), and are typically found as tandem duplicates in the genome (*dlx1* and *-2*, *dlx3* and *-4*, and *dlx5* and *-6*) (Stock et al., 1996). This paired genomic architecture arose from *cis*-duplication at the first *dlx* locus in the pre-vertebrate chordate lineage; this apparently occurred in stem olfactores (tunicates + vertebrates) after the divergence of cephalochordates (Wada and Makabe, 2006; Fig. 4). This paired architecture has been retained at most gnathostome *dlx* loci, but this arrangement has not been confirmed in cyclostomes for any of their six *dlx* loci. In early vertebrates, the first tandem pair underwent whole genome and/or regional *trans*-duplications (and potentially some losses) giving rise to the six genes we find in most modern vertebrate lineages (Stock, 2005; Takechi et al., 2013). It is important to note that despite cyclostomes and most gnathostomes having six main types of *dlx* genes, there is strong evidence that hagfish, lamprey, and gnathostome *dlx* genes are not all directly orthologous to each other (Cerny et al., 2010; Fujimoto et al., 2013; Kuraku et al., 2010; Stock, 2005; Takechi et al., 2013), although the exact history of duplication and retention is difficult to address in the face of differential paralog loss (Kuraku, 2013). The current *dlx* assemblages have thus arisen from some number of lineage-specific *trans*-duplications in each of these three groups.

In gnathostomes, tandem pairs of *dlx* genes typically share some aspects of their expression domains, although notably the *dlx1/4/6* group is consistently expressed in a more restricted manner than its tandem duplicate in the *dlx2/3/5* clade (Compagnucci et al., 2013; Depew et al., 2002; Gillis et al., 2013; Square et al., 2015; Talbot et al., 2010). This likely reflects a regulatory condition that arose at the

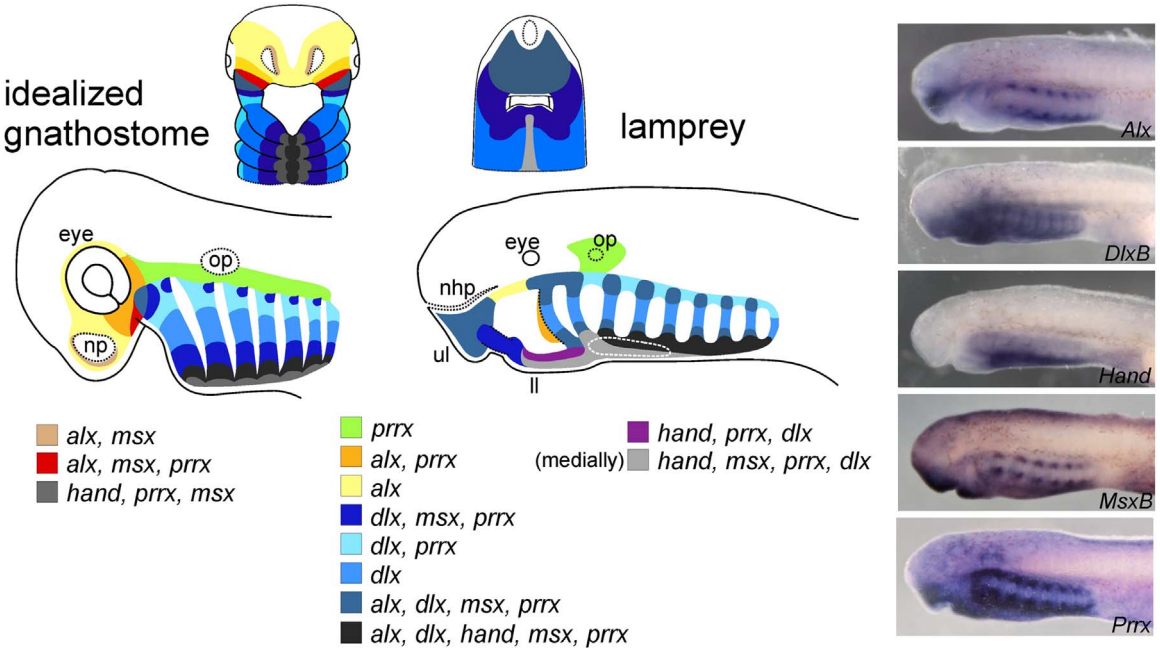

Fig. 3. A comparison of the gene expression schemes of lamprey and gnathostome nascent head skeletons. Top are oral views, below which are left lateral views. The key below is arranged such that the combinatorial domains in the left and right columns are found only in gnathostomes or lamprey, respectively, while the combinatorial domains in the middle column are found in both lineages. For gene types with multiple paralogs, these domains represent th expression of all paralogs (e.g. an *msx* positive domain could express multiple or any one of the *msx* genes in that lineage). On the right are example *in situ* hybridizations of each gene depicted in the lamprey expression map. The gnathostome map represents a simplification and slight modification to the map found in (Square et al., 2015). The ventrally-positioned white dotted oval in the lamprey represents the position of the endostyle, which is derived from endoderm and expresses none of the genes addressed here. ll, lower lip; nhp, nasohypophyseal plate; np, nasal placode; op, otic placode; ul, upper lip.

original *dlx1/4/6* and *dlx2/3/5* locus after the initial tandem duplication. In gnathostomes, some *dlx* functions are relegated to specific sets of *dlx* genes, such as *dlx2* in migratory CNCCs (Compagnucci et al., 2013; Crump et al., 2004; Square et al., 2015), *dlx2, -3, -4,* and *-5* in developing tooth germs (Borday-Birraux et al., 2006; Renz et al., 2011; Zhao et al., 2000), and *dlx1, -2, -5,* and *-6* in the forebrain (Renz et al., 2011; Zerucha et al., 2000). Subsets of lamprey *dlx* genes are also found in migrating CNCCs (*dlxA*, *-B*, *-C*, and *-D*), as well as the forebrain (*dlxA*, *-C*, *-D*, and *-E*) (Kuraku et al., 2010). Despite the ambiguity surrounding the exact level of gene orthology here, the presence of these specialized expression domains combined with information from phylogenetic analyses indicate that the full sets of lamprey and hagfish *dlx* genes do not stem from only within-cyclostome duplications (Fujimoto et al., 2013). Furthermore, recent evidence suggests that cyclostomes diverged after at least one whole genome duplication in vertebrates (Kuraku, 2013; Kuraku et al., 2009; Smith and Keinath, 2015), which is the process assumed to have given rise to the *trans*-duplication of *dlx* genes (Stock, 2005; Stock et al., 1996; Takechi et al., 2013). Thus, the vertebrate common ancestor likely had at least two pairs of *dlx* genes (Stock, 2005; Takechi et al., 2013; Fig. 4). It also seems most probable that these two pairs of *dlx* genes were differentially expressed in the vertebrate common ancestor given the high degree of specialization we see across all living vertebrate *dlx* complements.

At mid-pharyngula stages the *dlx* genes appear in nested PA expression domains in both sea lamprey (Cerny et al., 2010) and gnathostomes (Brown et al., 2005; Compagnucci et al., 2013; Depew et al., 2002; Gillis et al., 2013; Renz et al., 2011; Square et al., 2015; Talbot et al., 2010; Fig. 4). In both lineages, this nested pattern is deployed and refined soon after the CNCCs cease their migration, with the highest number of *dlx* paralogs consistently expressed in CNCCs occupying the intermediate and/or ventral-intermediate domain of the PAs. In gnathostomes, this nesting is referred to as the "*dlx* code" for its role in specifying identity along the dorsoventral axis in PA1 (a.k.a. the proximal/distal axis) (Depew et al., 2002). There is also strong evidence that hagfish *dlx* genes are at least expressed differentially in pre-skeletogenic mesenchyme (Fujimoto et al., 2013), though the presence or absence of nesting in the PAs remains to be addressed. Importantly, the CNCC population expressing the most *dlx* paralogs is generally situated more ventrally in gnathostomes as compared to the centrally-nested lamprey scheme, although the exact focal point of nesting seems to vary slightly between groups (Fig. 4). For example, most gnathostomes show distinct dorsal boundaries of *dlx3* and *dlx5* expression, though the amphibian *Xenopus laevis* shows a shared dorsal boundary of these two genes, making their dlx code more centered along the dorsoventral axis (Fig. S2).

There are many other lineage-specific modifications to the *dlx* code in gnathostome PAs, especially with regard to the *dlx1/4/6* group. To list a few examples: *Xenopus laevis dlx2* is absent from the dorsal PA2 (Square et al., 2015), mouse *dlx5* is expressed further ventrally (distally) than *dlx2* (Jeong et al., 2008), sharks exhibit an early restriction of *dlx1* to the dorsal PA1 (Compagnucci et al., 2013; Gillis et al., 2013), and reptilian *dlx4* seems to have been pseudogenized (Brown et al., 2005; Takechi et al., 2013). Furthermore, the posterior-most one to three PAs frequently show a delay or change in the dlx code in the pharyngula stages addressed here. This is likely due to either temporal differences in the specification of PA CNCCs, or simply degeneration of *dlx* expression in these less prolific PAs. Aside from these nuances, cyclostomes and gnathostomes still each possess three main *dlx*-positive domains in the PAs marked by different combinations of *dlx2/3/5* gene expression (Fig. 4).

Thus the common ancestor of all vertebrates likely also specified at least three different PA subdomains of CNCCs using a rudimentary *dlx* nesting scheme: the dorsal and ventral domains with transcripts from only one pair of *dlx*s, and an intermediate region with transcripts from two pairs of *dlx*s (Fig. 4). Given the important role of *dlx*s in specifying dorsoventral PA identity in zebrafish (Talbot et al., 2010) and mouse (Depew et al., 2002), it seems plausible that nested *dlx* expression has an ancient role in conferring position-specific skeletal morphology or histology that evolved before the appearance of PA subdivisions in gnathostomes, including the primary jaw joint in PA1. Comparative studies on *dlx* transcriptional regulation across vertebrates, including

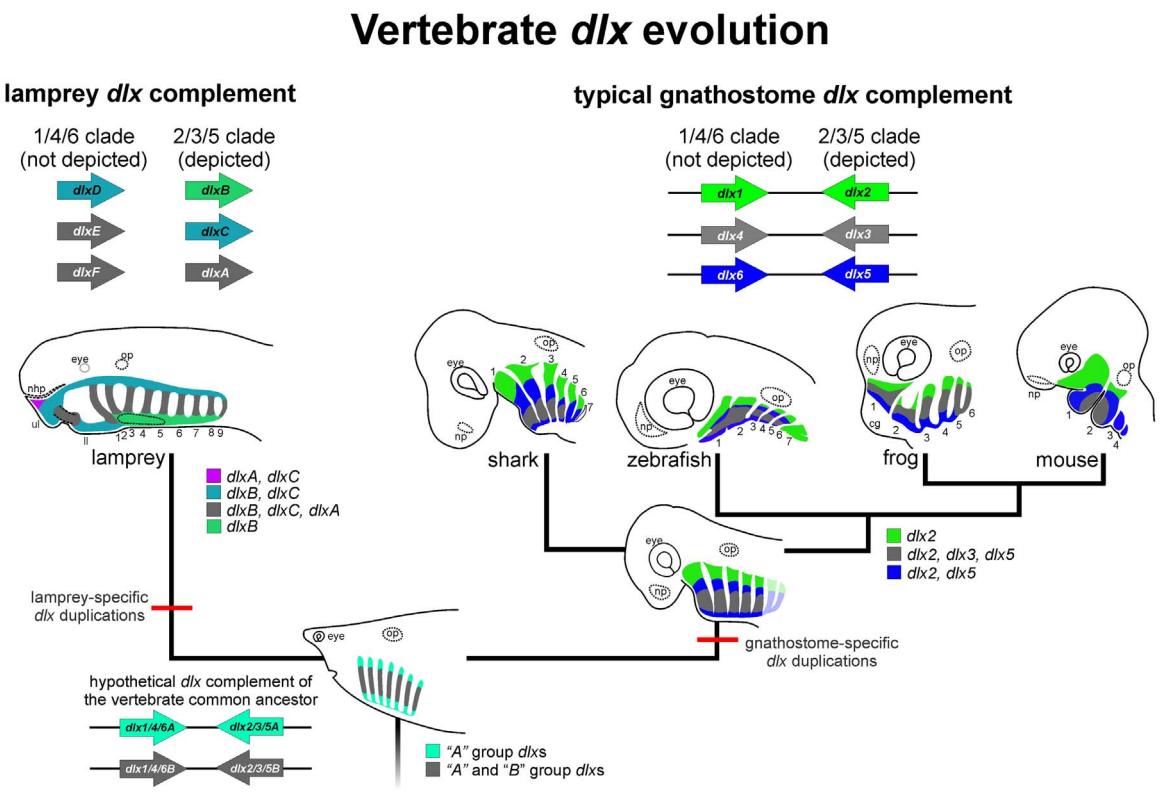

Fig. 4. *dlx* evolution in vertebrates. The colors of the genes are meant to reflect nested expression categories, rather than the relatedness of these genes, with the gray color being shared by all groups to indicate that all *dlx2/3/5* genes are expressed there. From bottom to top: The common ancestor to all living vertebrates likely had two pairs of *dlx* genes, which arose by first a *cis*-duplication, and later a *trans*-duplication (see *dlx* section in main text). Hypothesized *dlx* gene expression is depicted on a representation of this common ancestor's head skeleton, with all four genes expressed in the intermediate PAs (gray domain), and only one pair of *dlx* genes expressed throughout the PAs (turquoise domains). Thereafter (above), the modern cyclostome and gnathostome lineages diverged, each of which duplicated and retained at least two more *dlx* genes independently (thus lamprey and gnathostome *dlx* gene domains are colored differently, other than the gray domain where all six are expressed). Modern gnathostome *dlx* expression is depicted for a shark (*Scyliorhinus canicula*) (Compagnucci et al., 2013), zebrafish (*Danio rerio*) (Talbot et al., 2010), frog (*Xenopus laevis*) (Square et al., 2015), and mouse (*Mus musculus*) (Jeong et al., 2008). The 'average' of these four vertebrates is depicted below as an idealized gnathostome common ancestor. The ventrally-positioned black dotted oval in the lamprey represents the position of the endostyle, which is derived from endoderm and expresses no *dlx* genes. The PAs are numbered in each extant vertebrate at their base. ll, lower lip; nhp, nasohypophyseal plate; np, nasal placode; op, otic placode; ul, upper lip.

cyclostomes, should shed more light on ancestral vertebrate dlx expression.

Like the domains delineated by *alx, hand, msx,* and *prrx*, these main *dlx* domains do not seem to have a 1:1 correspondence with any skeletal elements, but instead mark groups of entire future elements, and occasionally parts of future elements, comprising larger-scale morphological modules (e.g. the many elements of the future lower jaw skeleton are marked by *dlx5* and *-6*). This is shown by vital dye labeling (Gillis et al., 2013), reporter expression (Ruest et al., 2003), and the functional transformation and truncation of multiple skeletal elements when *dlx* genes are perturbed (Depew et al., 2002; Talbot et al., 2010). Therefore, these *dlx* domains instead seem to grant a general identity to these different PA domains along the dorsoventral axis that contain the CNCCs belonging to multiple nascent skeletal elements.

3.4. Combinatorial gene expression defines conserved skeletal precursor populations outside of the PAs

Within gnathostomes are found four main groups of *alx* genes (*1–4*), though some of these have been lost in evolution by different groups (McGonnell et al., 2011). In lamprey only a single ortholog is known (Cattell et al., 2011). In addition to the PAs (discussed above), *alx* gene expression is found throughout the presumptive chondrocranium of gnathostomes, where these genes play critical roles in the differentiation of these non-PA skeletal structures (Antonopoulou et al., 2004; Beverdam et al., 2001; Beverdam and Meijlink, 2001; Compagnucci et al., 2013; Dee et al., 2013; McGonnell et al., 2011). Notably, these skeletal elements are composed of CNCCs, mesoderm, or a mix of both cell types, and the location of the 'boundary' between these two cell types seems to be somewhat plastic in evolution (Kague et al., 2012; Piekarski et al., 2014). Cyclostomes do possess cartilages dorsal to and surrounding the mouth, some of which comprise their neurocranium (Johnels, 1944; Oisi et al., 2013), though these individual skeletal elements lack obvious homology to the well-conserved set of gnathostome neurocranial elements. Even comparing lampreys and hagfishes does not reveal obvious affinities between these structures, though their genetic and developmental affinities can be addressed in this context (Kuratani et al., 2016). In lamprey, the 'trabecular' skeletal elements express *alx* during their development (Cattell et al., 2011). Lamprey and most gnathostomes thus have a domain near the eye that is *alx* positive, but *dlx*, *hand, msx*, and *prrx*-negative. Based on its conserved position and gene expression, we posit that this "*alx*-only" module (yellow in Fig. 3) is likely homologous between cyclostomes and gnathostomes, having been greatly expanded in the gnathostome lineage to form other components of the ventral braincase. Interestingly, this is one of the few head skeletal regions in lamprey that is thought to originate from mesoderm (Kuratani et al., 2016). This region of the lamprey head skeleton therefore may offer potential insights into the evolution of the braincase.

prrx genes are related to *alx* genes, but this duplication predates the divergence of echinoderms and chordates (Howard-Ashby et al., 2006), and thus these genes have diverged substantially in both their amino acid sequences and their expression patterns. In gnathostomes are two *prrx* genes, though both seem to have very similar expression patterns. We identified a single *prrx* gene transcript in lamprey, which according

to phylogenetic analysis is the outgroup to all gnathostome Prrxs (Fig. S3). As in gnathostomes, this *P. marinus prrx* gene is expressed in a mesenchymal domain near the otic placode (green in Fig. 3) which likely gives rise to the otic capsule (ten Berge et al., 1998). Around the mouth, all vertebrates addressed also have a single region where *alx* and *prrx* are coexpressed in the absence of any *dlx, hand,* or *msx* gene. In lamprey, this *alx+prrx* module becomes the medial velar skeleton (the opposable "flap" of the velum; orange in Fig. 4), while in gnathostomes this domain is found within the future chondrocranium, lateral to the future palate and below/partially surrounding the eye. This region is not part of the gnathostome PAs, but still receives a CNCC contribution. Thus in both lineages, this *alx+prrx* module is adjacent to and strongly associated with PA1, but has a distinct expression profile compared to PA tissue, namely in that it is *dlx*-negative (Square et al., 2015; Kuraku et al., 2010). In lamprey, the position and function of the medial velar skeleton suggests it is derived from PA1, however upon closer inspection this structure also shows a clear histological association to the more dorsal 'chondrocranial region' near the notochord (Fig. S4). This and its lack of *dlx* expression indicate that it might instead be derived from non-PA CNCCs or mesoderm of the rudimentary lamprey "chondrocranium".

3.5. Nested hox expression defines PA identities in all living vertebrates

Aside from within-PA patterning, nested *hox* gene expression in the pharynx along the anteroposterior axis occurs in both lampreys and gnathostomes; these expression patterns were recently shown to be deployed via conserved regulatory machinery (Parker et al., 2014). As in other tissues, these expression patterns are collinear, and confer each PA with a unique *hox* identity. In all modern vertebrates, pre-oral and PA1 mesenchyme is *hox*-negative, PAs 2+ are *hox2* positive, and PAs 3+ are *hox3* positive (Hunt et al., 1991a, 1991b, 1991c; Lyon et al., 2013; Minoux et al., 2009; Takio et al., 2007). Interestingly, these highly conserved *hox* domains correspond to the three migrating populations of CNCCs (discussed above), and generally reflect the expression profile of the brain region they delaminate from (Parker et al., 2016). In gnathostomes, this expression confers PA-specific morphology: exogenous or depleted Hox function can lead to homeotic transformations of the PAs (reviewed by Minoux et al. (2009)), however no work on any cyclostome Hox function has been published to date. Both lamprey and gnathostomes also have at least one other hox gene expressed in a subset of more posterior arches, though the similarity is not as strong: the arctic lamprey expresses *Hox4x* in a gradient from posterior to anterior (Takio et al., 2007), whereas gnathostomes show clearer nesting of *hox4* in PAs 4+(Lyon et al., 2013; Minoux et al., 2009), and *hox5* in PAs 5+(if present) (Lyon et al., 2013). It is useful to note that, like the *dlx* genes, *hox* genes have undergone multiple *trans*-duplications in vertebrate lineages due to whole genome and other large-scale duplications (Smith and Keinath, 2015), and each modern *hox* cluster seems to have nuanced expression between gnathostome groups (Hunt et al., 1991a, 1991b, 1991c; Lyon et al., 2013; Minoux et al., 2009). Despite this, we can still safely deduce that the vertebrate common ancestor deployed *hox2*, *hox3*, and *hox4* genes in the PAs to confer specific transcriptional identities to CNCCs of the nascent viscerocranium, with PA1 and pre-oral CNCCs specifically being *hox*-negative.

In the *hox*-negative pre-oral and PA1 mesenchyme of lamprey and gnathostomes (derived from the 1st stream of CNCCs), *otx* is uniquely transcribed prior to CNCC migration (Acampora et al., 1995; Tomsa and Langeland, 1999; Zhang et al., 2014). Thus an '*otx* and *hox*' CNCC patterning scheme has been suggested to encompass all PAs, with *otx* in first stream CNCCs being implicated as a possible avenue for jaw evolution (Kuratani, 2004). Importantly, the role of *otx* in this tissue seems to strongly differ from *hox* in that this expression is not maintained throughout most 1st stream migratory or post-migratory skeletogenic CNCCs. At the pharyngula stages when we find persisting *hox* expression in PAs 2+, the majority of PA1 and pre-oral mesenchyme is *otx*-negative. In all vertebrates addressed to date, *otx* is found in a small subset of migratory and post-migratory CNCCs (Kudoh et al., 2001; Matsuo et al., 1995; Tomsa and Langeland, 1999; Zhang et al., 2014), which usually appears to correspond to CNCC-derived ganglia. To our knowledge, the function of *otx* in craniofacial skeletogenesis has been addressed only in the mouse (Matsuo et al., 1995), however, the knockout method used does not separate this gene's potential role in general CNCC specification from a possible later role in the identity of anterior ectomesenchyme, unlike some temporally-inducible *hox* experiments performed in *Xenopus* and mouse (Pasqualetti et al., 2000; Santagati et al., 2005). Thus PA1 truncations and deformities seen in *otx*-null or heterozygous mice might simply arise from the improper specification of the neural plate and neural plate border (including premigratory CNCCs) at the position of the anterior midbrain rather than a more specific perturbance in the skeletal identity of PA1 and pre-oral CNCCs. Furthermore, no homeotic transformation or suggestion of a different identity was seen in these mutants; only a truncation or absence of certain skeletal elements. Thus, while *otx* might have a deeply conserved, early role in 1st stream CNCC differentiation via specification of anterior neural tissues, this function appears to be more general, and occurs distinctly earlier than *hox* gene function in post-migratory skeletogenic CNCCs.

3.6. Differences in transcription factor expression between cyclostomes and gnathostomes in the nascent head skeleton

While there are many similarities in gene expression in the head skeletal precursors of lamprey and gnathostomes, there are also some clear differences. Lacking an appropriate living outgroup for rooting these comparisons, these differences could reflect gain, modification, or loss in either the gnathostome or cyclostome lineages. Thus, despite gross similarity between lamprey larvae and fossils of early vertebrate relatives, it should not be automatically assumed that a trait is ancestral if it is present in lamprey but not gnathostomes.

The *dlx* genes, though nested in lampreys and gnathostomes, show some definite differences in expression between these two major groups. The presence of a *dlx*-negative ventralmost domain in gnathostomes (Compagnucci et al., 2013; Jeong et al., 2008) is not mirrored in lampreys (Cerny et al., 2010), where *dlxB* is expressed throughout the ventralmost extent of ectomesenchyme in the head (below the endostyle). This might somehow relate to the differences in morphology of these ventral PAs between both lineages, where lampreys have no distinct ventral cartilage elements but gnathostomes have medial basibranchials and a basihyal that are composed of CNCCs derived from both the left and right sides of the head. Outside the PAs, an interesting and previously noted difference between gnathostomes and cyclostomes is the presence of *dlx*-positive pre-oral mesenchyme in the latter (Kuratani et al., 2013; Shigetani et al., 2002). Mesenchyme in this region of the lamprey head has an expression profile more similar to the oro-maxillary region in gnathostomes (dorsal/proximal PA1). This difference between lamprey and gnathostomes has been hypothesized to stem from a heterotopic shift in the signals received by the CNCCs in the oral region (Kuratani et al., 2013; Shigetani et al., 2002), which could have changed the locations at which CNCCs were induced to have a *dlx*-positive expression profile. However with no appropriate outgroup, whether this pre-oral dlx expression is ancestral and lost in gnathostomes or a derived expression gain in lampreys will remain difficult to address.

goosecoid (*gsc*) genes exhibit unique expression profiles across vertebrates (Cerny et al., 2010; Gaunt et al., 1993; Schultemerker et al., 1994; Square et al., 2015), but are expressed within the same broad populations of ectomesenchyme. In the early pharynx, this gene's expression is relegated to mainly to PA1, PA2, and a subset of non-PA mesenchyme just ventral to the brain in all lineages. However even

within gnathostomes, *gsc* expression is plastic, exhibiting clear differences between different major groups. For example, zebrafish *gsc* transcription is observed in dorsal PA1 (Schultemerker et al., 1994), but this domain is not reflected in any other gnathostome addressed to date. Generally speaking, in gnathostomes this gene is expressed in the ventral PA1 and PA2, and also in mesenchyme of the future ventral chondrocranium (beneath the eye, near the palate). Lamprey also expresses *gsc* intricately in PA1, PA2, and the upper lip, although this gene is essentially absent from the ventralmost domain, save a small spot of expression in the distalmost lower lip (Cerny et al., 2010). So, overall, it seems that *gsc* has an ancient role in specializing the regional expression profiles of at least PA1, PA2, and some subset of dorsal or pre-oral non-PA mesenchyme in vertebrates, though the precise expression pattern of *gsc* in the vertebrate common ancestor is unclear.

Lamprey expresses *alx* in the dorsal and ventral portions of most PAs (Cattell et al., 2011), similar to *prrx* expression (Fig. 3, Fig. S1). This set of *alx* expression domains is not seen in any extant gnathostome addressed to date, which instead express *alx* genes only in the ventral PAs and chondrocranium adjacent to the dorsal PAs (Beverdam and Meijlink, 2001; Cattell et al., 2011; Compagnucci et al., 2013; Dee et al., 2013; McGonnell et al., 2011; Square et al., 2015). Interestingly, *alx* and *prrx* are related genes; thus if preexisting gene regulatory machinery was coopted for these pharyngeal expression domains, the *alx*-negative dorsal PAs in gnathostomes might reflect a loss of expression in the ancestral gnathostome *alx* gene, with *prrx* having retained this expression. Given that some expression is conserved between *alx* and *prrx*, this notion could be tested by work on *alx* and *prrx* gene regulation in both gnathostomes and cyclostomes.

Other genes that are expressed dissimilarly in lamprey and gnathostomes include *nkx3.2* (*bapx*) (Cerny et al., 2010; Nichols et al., 2013), *barx* (Cerny et al., 2010; Nichols et al., 2013), *mef2* (Jandzik et al., 2014), and *emx* (Fig. S1). These genes offer a range of observable differences: some are found in mesenchyme with different skeletogenic potentials (*barx*), CNCCs in dissimilar locations (*nkx3.2*), or absent from CNCCs in lamprey (*emx* and *mef2*). In the case of lamprey *emxA*, it would appear that the dorsoventral cue that positions the expression in the pharynx might be conserved with *emx2* (an "intermediate" PA patterning gene in gnathostome CNCCs), but the lamprey ortholog is being deployed in epithelial ectoderm and endoderm instead of the future skeleton (Fig. S1). Similarly, lamprey *barx* is found in the innermost, CNCC-derived mesenchyme of the PAs (nearest the cavity of the pharynx), but this tissue does not give rise to larval skeletal elements. With some functional assays, these curious differences in expression might offer clues as to how these genes are activated, and thus allow us to understand how cyclostomes and gnathostomes become so different both morphologically and histologically during development.

4. The early vertebrate head: general characteristics and evolutionary trends

Fossilized early vertebrate relatives such as *Haikouella* (Mallatt and Chen, 2003), *Haikouichthys* (Shu et al., 1999, 2003), *Myllokunmingia* (Shu et al., 1999), and *Metaspriggina* (Morris and Caron, 2014) arose during the early to mid-Cambrian, and are generally assumed to predate the most recent common ancestor of all living vertebrates. While phylogenies based on available character states usually place these fossil animals at the base of all vertebrates, there is some uncertainty: occasionally these fossils show a greater affinity for gnathostomes, lampreys, or hagfish, depending on tree reconstruction parameters and the traits chosen for analysis (Mallatt and Chen, 2003; Morris and Caron, 2014; Sansom et al., 2010; Shu et al., 1999). Regardless of disagreements over their exact phylogenetic position (Donoghue and Purnell, 2009; Gess et al., 2006; Morris and Caron, 2014; Sansom et al., 2010; Shu et al., 1999, 2003), these fossils inform us as to the timing of evolutionary events, confirming that a given character state had arisen by a given epoch.

Like modern lamprey larvae, all of the aforementioned fossil vertebrate relatives appear to have possessed a cartilaginous endoskeleton composed mainly of simple pharyngeal cartilage rods (within the PAs), with some oral and/or cranial chondroid tissue (Mallatt and Chen, 2003; Morris and Caron, 2014; Shu et al., 1999, 2003). Dissimilar to this condition, hagfishes display extremely derived reduction of the pharyngeal skeleton, having apparently lost all but two of their branchial arches despite still possessing a high number of gill slits (between 6 and 12 pairs). Despite their reduced number, hagfish branchial arch cartilages are also fused to the rest of their head skeleton like in lampreys, in a basket-like condition (albeit a small basket) (Oisi et al., 2013). Notably, the fossilized cartilage bars found in specimens such as *Metaspriggina* (Morris and Caron, 2014) and *Haikouichthys* (Shu et al., 2003) do not appear to be connected by dorsal and ventral horizontal bars, nor are they juxtaposed at their apices, suggesting the fused branchial basket might be a derived character of cyclostomes. Like most modern gnathostomes, the recently reported Cambrian fossil *Metaspriggina* (Morris and Caron, 2014) also appears to have distinct dorsal and ventral PA skeletal elements. If *Metaspriggina* diverged before the gnathostome and cyclostome lineages split, this would raise the possibility that cyclostomes acquired single vertical rods in each PA by secondarily fusing ancestrally separate dorsal and ventral skeletal elements. Interestingly, modern anurans possess both of these cyclostome-like characters in their branchial arches: these lack any dorsoventral segregation, and are also fused at their apices in a basket-like condition (Rose, 2014). Together, this could explain why lamprey has gnathostome-like patterning of its skeletal primordia, while also forming contiguous rods in each PA: despite reverting to a fused morphology, the patterning scheme is mostly retained (Cerny et al., 2010) (as is also seen in *Xenopus* branchial arches (Square et al., 2015)). An alternative hypothesis is that cyclostomes and gnathostomes diverged earlier than presumed, and *Metaspriggina* split from the lineage leading to gnathostomes after the evolution of distinct dorsal and ventral skeletal elements in that lineage. It is also possible that *Metaspriggina* and gnathostomes independently acquired separate dorsal and ventral elements. Regardless of the precise scenario, the presence of gene expression reminiscent of the gnathostome condition in the developing lamprey head skeleton and the bipartite pharyngeal skeleton of *Metaspriggina* strongly support the idea that the developmental mechanisms needed to distinguish the dorsal from ventral pharyngeal skeleton precursors predate jaws by 100 million years or more.

Looking above the PAs, one general trend in vertebrate head skeletal evolution was the expansion of the chondrocranium (forming the brain case, or neurocranium), which does not seem to be prominent in the earliest vertebrate fossils, if present at all (Mallatt and Chen, 2003; Morris and Caron, 2014; Shu et al., 1999, 2003). In modern gnathostomes, these more dorsal structures are partially or sometimes largely derived from mesoderm, unlike the facial skeleton and PAs (the viscerocranium) which are mainly derived from CNCCs (Kague et al., 2012; Piekarski et al., 2014). While cyclostomes have small cartilages near the brain, including "trabeculae", these do not have any clear structural homology to any specific gnathostome cartilages, though it is suggested by their general position (Kuratani et al., 2016). Nevertheless, a prominent and three-dimensionally complex ethmoid/trabecular skeleton and the presence of an extensive braincase are clearly derived characters of the gnathostome group. This means that the head skeleton of the vertebrate common ancestor was composed of mainly PAs and some oral-associated mesenchyme, the majority of which were probably derived from CNCCs, similar to the condition in modern lampreys.

Cyclostomes and the earliest fossil vertebrate relatives lack cranial bones (or any bones for that matter), which first appear in the fossil record in jawless vertebrates of the subclass Pteraspidomorphi (Janvier, 1996; Fig. 1). This means that the embryonic cartilaginous

head endoskeleton in bony vertebrates (osteichthyans) is more similar compositionally to the earliest vertebrate head skeletons, rather than the adult bony fish head skeleton, which comprises mainly dermal bones with some ossified elements of the endoskeleton. However, it is interesting to note that in modern osteichthyans, many bones of the head develop from the same pool of CNCCs that give rise to the larval cartilaginous head skeleton (Hirasawa and Kuratani, 2015). Importantly, some key aspects of genetic patterning that occur within the common progenitor pool of CNCCs affect the initial larval head skeleton as well as the later ossified skeleton, such as the *dlx* (Depew et al., 2002) and *hox* (Minoux et al., 2009) codes. So despite the striking histological and morphological differences between a given osteichthyan's larval and adult head skeletons, these two complex structures are strongly tied to each other developmentally. Thus, the patterning schemes described here presumably have effects on all modern head skeletons, both larval and adult.

5. Differences in vertebrate head skeletons

What is the output of this extensive patterning via transcription factor expression? Given that these modules do not correspond to individual skeletal elements in gnathostomes, and head skeleton elements are histologically contiguous in cyclostomes, the relationship between this patterning scheme and eventual skeletal morphology is quite abstracted, i.e. there is poor correspondence in shape and size between individual gene regulatory modules (like those shown in Fig. 3) and the delineation of cartilage and/or bony elements that will arise from a given region later in development. All modern vertebrate head skeletons are very complex, displaying intricate three dimensional structure within skeletal elements, and also with respect to the juxtaposition of these elements. In order to generate any sort of three-dimensional variety in a given skeletal region, this requires that cells within a given primordium divide at a different rate or on a different axis than cells in other primordia, or in other parts of the same primordium (Kimmel et al., 1998). While some studies are beginning to understand how cell division is controlled to these ends in the head skeleton (Le Pabic et al., 2014), much work is still needed to place these events within the context of vertebrate transcription factor patterning in the head. In gnathostomes, mutations in the transcription factors that pattern head skeleton precursors cause the loss of joints as well as changes in the shape of skeletal elements, showing that these patterning genes drive some part of both the overall shape and composition of the head skeleton. With modern developmental genetic tools, the processes linking early patterning to later cell division and histological composition will become more evident.

One general difference between cyclostomes and gnathostomes relates to the high level of dorsoventral symmetry in transcription factor expression within posterior lamprey PAs as compared to gnathostomes. Interestingly, in lamprey, this symmetry starts at the level of gene expression (Fig. 3), and is later reflected in their highly symmetrical pharyngeal basket. Gnathostomes instead have more polarized PAs with respect to both gene expression and eventual morphology. This is at least in part dictated by the ventral secretion of Edn1 protein in gnathostomes, which works to specify the ventral and intermediate domains. Conversely, no sea lamprey *edn* ligand is restricted to all or most ventral PAs; instead, *ednA* and *ednE* transcripts are found in a more centralized pattern in the PAs (Square et al., 2016), removing the possibility that any *edn* ligands in sea lamprey work as ventral specifiers as they do in gnathostomes. We speculate that the level of symmetry in these gene expression domains might somehow contribute to the symmetry of the lamprey pharyngeal basket by driving a similar identity, and thus morphology of these domains in lamprey (namely the dark blue *alx, dlx, msx, prrx* domains in Fig. 3). More functional studies in cyclostomes are needed to link head skeleton gene expression and morphology, but in gnathostomes the *dlx* genes alone have been shown to drive the general identity of entire regions of PAs, which supports this notion given the expression patterns known across vertebrates (Fig. 4).

Another obvious aspect of derived morphology is the specialization of the oral skeleton (pre-oral mesenchyme, PA1, and PA2) in all modern vertebrate lineages. In lamprey, oral skeletogenic mesenchyme gives rise to the oral hood, velum, and elongated lower lip, whereas in gnathostomes it forms the mandible, maxilla, palate and nasal region. How these differentiated structures are related to each other has been a topic of debate for more than a century. Despite striking differences in final morphology, developmental gene expression has the potential to show how the precursor cell populations that generate disparate skeletal structures might be related, at least on the level of transcriptional identity. The lamprey upper lip is a skeletal element positioned just rostral to the mouth, similar to the maxillary/nasal elements of the gnathostome head skeleton. Despite this spatial similarity, nearly the entire lamprey upper lip has a transcriptional identity similar to the dorsalmost anterior PA1 of gnathostomes, while most of the lower lip has the transcriptional identity of the gnathostome ventral PA1. Interestingly, the lower lip demonstrates an anterior expansion perpendicular to the dorsoventral axis of PA1, rather than an extension ventrally/distally with a bent axis.

The head skeletons of both gnathostomes and cyclostomes are composed of multiple morphologically distinct skeletal elements (though these elements are connected in cyclostomes), and several histologically distinct skeletal tissue types (Cattell et al., 2011). These include joint tissue in gnathostomes, various types of mucocartilage in lampreys, and soft and rigid collagen-containing, proteoglycan-rich cellular cartilage in both groups. Future work in both gnathostomes and cyclostomes will help elucidate if the conserved targets of the genes that confer these local transcriptional identities include structural genes such as collagens, lecticans, and glypicans.

Based on work in gnathostomes, it is likely that patterning via transcription factor expression in stem vertebrates provided a framework for position-specific morphogenesis and tissue differentiation, though precisely how this occurred is unclear. Given the conserved aspects of early head skeleton development, it is likely changes developmentally downstream of genes such as *hox, alx, dlx, hand, msx,* and *prrx* were major players in the generation of the different major vertebrate forms. These genes' expression patterns seem to have evolved prior to the most recent common ancestor of all living vertebrates – at least in large part. However, the nuanced differences we do see in these genes might contribute to large differences amongst vertebrates in the shape or composition of some regions of the head skeleton, such as less symmetrical *alx* in the gnathostome PAs, or *dlx* expression in the lamprey upper lip.

6. Conclusion

Based on detailed comparisons of living jawed and jawless vertebrates, it is likely that the head skeleton of the most recent common ancestor of all living vertebrates formed mainly from CNCCs. These cells migrated as three molecularly distinct populations, and expressed a core set of chondrogenic transcription factors. After migration into the oropharyngeal region, those cells activated a set of transcription factors which conferred regional identities upon different skeletal precursor subpopulations along multiple axes, including a set of at least 10 transcription factors (*hox1*, *hox2*, *hox3*, *hox4*, *dlx2/3/5A*, *dlx2/3/5B*, *alx*, *hand*, *msx*, and *prrx*). Similarities in this head skeleton patterning system across jawed and jawless vertebrates likely reflect homology of many of these precursor subpopulations, but it is important to recognize that these regulatory cassettes could be deployed in new regions of the head, in which case it would be more appropriate to consider them deeply homologous (see Shubin et al. (2009)). It is unclear, however, if the specific skeletal structures derived from these developmental units should be considered homologous *sensu stricto*, even if they are similarly juxtaposed with other elements

and tissues in the head. By further dissecting the gene expression and function of different genes in different lineages, we will continue to build our understanding of what all heads share, how they are developmentally constrained, and also how genetic changes underlie changes in morphology.

Acknowledgements

We thank Jr-Kai Yu for kindly inviting us to contribute to this special issue, Haley Stein for assistance with *in situ* hybridizations, Pei-San Tsai and Scott Kavanaugh for assistance with cryosectioning, and David Stock for his perspectives and advice on the manuscript. We also thank two anonymous reviewers, whose comments improved the work. T.S., D.J., M. R., and D.M.M. were supported by NSF grants IOS 0920751 and IOS 1257040. R. C. and M. R. were supported by the Czech Science Foundation (16-23836S) and by a Specific Research Grant from Charles University (SVV 260 313/2016).

Appendix A. Supplementary material

Supplementary data associated with this article can be found in the online version at doi:10.1016/j.ydbio.2016.11.014.

References

Acampora, D., Mazan, S., Lallemand, Y., Avantaggiato, V., Maury, M., Simeone, A., Brulet, P., 1995. Forebrain and midbrain regions are deleted in otx2(-/-) mutants due to a defective anterior neuroectoderm specification during gastrulation. Development 121, 3279–3290.

Antonopoulou, I., Mavrogiannis, L.A., Wilkie, A.O.M., Morriss-Kay, G.M., 2004. Alx4 and Msx2 play phenotypically similar and additive roles in skull vault differentiation. J. Anat. 204, 487–499.

Beverdam, A., Brouwer, A., Reijnen, M., Korving, J., Meijlink, F., 2001. Severe nasal clefting and abnormal embryonic apoptosis in Alx3/Alx4 double mutant mice. Development 128, 3975–3986.

Beverdam, A., Meijlink, F., 2001. Expression patterns of group-I aristaless-related genes during craniofacial and limb development. Mech. Dev. 107, 163–167.

Borday-Birraux, V., Van der Heyden, C., Debiais-Thibaud, M., Verreijdt, L., Stock, D.W., Huysseune, A., Sire, J.Y., 2006. Expression of Dlx genes during the development of the zebrafish pharyngeal dentition: evolutionary implications. Evol. Dev. 8, 130–141.

Brown, S.T., Wang, J.M., Groves, A.K., 2005. Dlx gene expression during chick inner ear development. J. Comp. Neurol. 483, 48–65.

Campo-Paysaa, F., Jandzik, D., Takio-Ogawa, Y., Cattell, M.V., Neef, H.C., Langeland, J.A., Kuratani, S., Medeiros, D.M., Mazan, S., Kuraku, S., Laudet, V., Schubert, M., 2015. Evolution of retinoic acid receptors in chordates: insights from three lamprey species, Lampetra fluviatilis, Petromyzon marinus, and Lethenteron japonicum. Evodevo 6.

Cattell, M., Lai, S., Cerny, R., Medeiros, D.M., 2011. A new Mechanistic scenario for the origin and evolution of vertebrate cartilage. PLoS One 6.

Cerny, R., Cattell, M., Sauka-Spengler, T., Bronner-Fraser, M., Yu, F., Medeiros, D.M., 2010. Evidence for the prepattern/cooption model of vertebrate jaw evolution. Proc. Natl. Acad. Sci. USA 107, 17262–17267.

Cerny, R., Meulemans, D., Berger, J., Wilsch-Brauninger, M., Kurth, T., Bronner-Fraser, M., Epperlein, H.H., 2004. Combined intrinsic and extrinsic influences pattern cranial neural crest migration and pharyngeal arch morphogenesis in axolotl. Dev. Biol. 266, 252–269.

Charite, J., McFadden, D.G., Merlo, G., Levi, G., Clouthier, D.E., Yanagisawa, M., Richardson, J.A., Olson, E.N., 2001. Role of Dlx6 in regulation of an endothelin-1-dependent, dHAND branchial arch enhancer. Genes Dev. 15, 3039–3049.

Compagnucci, C., Debiais-Thibaud, M., Coolen, M., Fish, J., Griffin, J.N., Bertocchini, F., Minoux, M., Rijli, F.M., Borday-Birraux, V., Casane, D., Mazan, S., Depew, M.J., 2013. Pattern and polarity in the development and evolution of the gnathostome jaw: both conservation and heterotopy in the branchial arches of the shark, Scyliorhinus canicula. Dev. Biol. 377, 428–448.

Crump, J.G., Maves, L., Lawson, N.D., Weinstein, B.M., Kimmel, C.B., 2004. An essential role for Fgfs in endodermal pouch formation influences later craniofacial skeletal patterning. Development 131, 5703–5716.

Dee, C.T., Szymoniuk, C.R., Mills, P.E.D., Takahashi, T., 2013. Defective neural crest migration revealed by a Zebrafish model of Alx1-related frontonasal dysplasia. Hum. Mol. Genet. 22, 239–251.

Delarbre, C., Gallut, C., Barriel, V., Janvier, P., Gachelin, G., 2002. Complete mitochondrial DNA of the hagfish, Eptatretus burgeri: the comparative analysis of mitochondrial DNA sequences strongly supports the cyclostome monophyly. Mol. Phylogenetics Evol. 22, 184–192.

Depew, M.J., Lufkin, T., Rubenstein, J.L.R., 2002. Specification of jaw subdivisions by Dix genes. Science 298, 381–385.

Donoghue, P.C.J., Purnell, M.A., 2009. Distinguishing heat from light in debate over controversial fossils. Bioessays 31, 178–189.

Firulli, A.B., 2003. A HANDful of questions: the molecular biology of the heart and neural crest derivatives (HAND)-subclass of basic helix-loop-helix transcription factors. Gene 312, 27–40.

Fujimoto, S., Oisi, Y., Kuraku, S., Ota, K.G., Kuratani, S., 2013. Non-parsimonious evolution of hagfish Dlx genes. BMC Evolut. Biol. 13.

Gans, C., Northcutt, R.G., 1983. Neural crest and the origin of vertebrates – a new head. Science 220, 268–273.

Gaunt, S.J., Blum, M., Derobertis, E.M., 1993. Expression of the mouse goosecoid gene during mid-embryogenesis may mark mesenchymal cell lineages in the developing head, limbs and body wall. Development 117, 769–778.

Gess, R.W., Coates, M.I., Rubidge, B.S., 2006. A lamprey from the Devonian period of South Africa. Nature 443, 981–984.

Gillis, J.A., Modrell, M.S., Baker, C.V.H., 2013. Developmental evidence for serial homology of the vertebrate jaw and gill arch skeleton. Nat. Commun. 4.

Heimberg, A.M., Cowper-Sallari, R., Semon, M., Donoghue, P.C.J., Peterson, K.J., 2010. microRNAs reveal the interrelationships of hagfish, lampreys, and gnathostomes and the nature of the ancestral vertebrate. Proc. Natl. Acad. Sci. USA 107, 19379–19383.

Hernandez-Vega, A., Minguillon, C., 2011. The Prx1 limb enhancers: targeted gene expression in developing zebrafish pectoral fins. Dev. Dyn. 240, 1977–1988.

Hildebrand, M., Goslow, G.E., 2001. Analysis of Vertebrate Structure 5th ed.. John Wiley, New York.

Hirasawa, T., Kuratani, S., 2015. Evolution of the vertebrate skeleton: morphology, embryology, and development. Zoological Lett. 1, 2. http://dx.doi.org/10.1186/s40851-014-0007-7.

Howard-Ashby, M., Materna, S.C., Brown, C.T., Chen, L., Cameron, R.A., Davidson, E.H., 2006. Identification and characterization of homeobox transcription factor genes in Strongylocentrotus purpuratus, and their expression in embryonic development. Dev. Biol. 300, 74–89.

Hunt, P., Gulisano, M., Cook, M., Sham, M.H., Faiella, A., Wilkinson, D., Boncinelli, E., Krumlauf, R., 1991a. A distinct hox code for the branchial region of the vertebrate head. Nature 353, 861–864.

Hunt, P., Whiting, J., Muchamore, I., Marshall, H., Krumlauf, R., 1991b. Homeobox genes and models for patterning the hindbrain and branchial arches. Development, 187, (&).

Hunt, P., Wilkinson, D., Krumlauf, R., 1991c. Patterning the vertebrate head - murine hox-2 genes mark distinct subpopulations of premigratory and migrating cranial neural crest. Development 112, 43–50.

Jandzik, D., Garnett, A.T., Square, T.A., Cattell, M.V., Yu, J.-K., Medeiros, D.M., 2015. Evolution of the new vertebrate head by co-option of an ancient chordate skeletal tissue. Nature 518, 534–537.

Jandzik, D., Hawkins, M.B., Cattell, M.V., Cerny, R., Square, T.A., Medeiros, D.M., 2014. Roles for FGF in lamprey pharyngeal pouch formation and skeletogenesis highlight ancestral functions in the vertebrate head. Development 141, 629–638.

Janvier, P., 1996. Early Vertebrates. Clarendon Press, New York.

Jeong, J., Li, X., McEvilly, R.J., Rosenfeld, M.G., Lufkin, T., Rubenstein, J.L.R., 2008. Dlx genes pattern mammalian jaw primordium by regulating both lower jaw-specific and upper jaw-specific genetic programs. Development 135, 2905–2916.

Johnels, A., 1944. On the cartilage and mucocartilage of the Petromyzon larva. Acta Zool. 25.

Kague, E., Gallagher, M., Burke, S., Parsons, M., Franz-Odendaal, T., Fisher, S., 2012. Skeletogenic Fate of Zebrafish Cranial and Trunk Neural Crest. PLoS One 7.

Kimmel, C.B., Miller, C.T., Kruze, G., Ullmann, B., BreMiller, R.A., Larison, K.D., Snyder, H.C., 1998. The shaping of pharyngeal cartilages during early development of the zebrafish. Dev. Biol. 203, 245–263.

Kudoh, T., Tsang, M., Hukriede, N.A., Chen, X.F., Dedekian, M., Clarke, C.J., Kiang, A., Schultz, S., Epstein, J.A., Toyama, R., Dawid, I.B., 2001. A gene expression screen in zebrafish embryogenesis. Genome Res. 11, 1979–1987.

Kuraku, S., 2013. Impact of asymmetric gene repertoire between cyclostomes and gnathostomes. Semin. Cell Dev. Biol. 24, 119–127.

Kuraku, S., Meyer, A., Kuratani, S., 2009. Timing of genome duplications relative to the origin of the vertebrates: did cyclostomes diverge before or after? Mol. Biol. Evol. 26, 47–59.

Kuraku, S., Takio, Y., Sugahara, F., Takechi, M., Kuratani, S., 2010. Evolution of oropharyngeal patterning mechanisms involving Dlx and endothelins in vertebrates. Dev. Biol. 341, 315–323.

Kuratani, S., 2004. Evolution of the vertebrate jaw: comparative embryology and molecular developmental biology reveal the factors behind evolutionary novelty. J. Anat. 205, 335–347.

Kuratani, S., Adachi, N., Wada, N., Oisi, Y., Sugahara, F., 2013. Developmental and evolutionary significance of the mandibular arch and prechordal/premandibular cranium in vertebrates: revising the heterotopy scenario of gnathostome jaw evolution. J. Anat. 222, 41–55.

Kuratani, S., Oisi, Y., Ota, K.G., 2016. Evolution of the vertebrate Cranium: viewed from Hagfish developmental studies. Zool. Sci. 33, 229–238.

Kuratani, S., Horigome, N., Ueki, T., Aizawa, S., Hirano, S., 1998a. Stereotyped axonal bundle formation and neuromeric patterns in embryos of a cyclostome, Lampetra japonica. J. Comp. Neurol. 391, 99–114.

Kuratani, S., Ueki, T., Hirano, S., Aizawa, S., 1998b. Rostral truncation of a cyclostome, Lampetra japonica, induced by all-trans retinoic acid defines the head/trunk interface of the vertebrate body. Dev. Dyn. 211, 35–51.

Le Pabic, P., Ng, C., Schilling, T.F., 2014. Fat-Dachsous signaling coordinates cartilage differentiation and polarity during craniofacial development. PLoS Genet. 10.

Lyon, R.S., Davis, A., Scemama, J.L., 2013. Spatio-temporal expression patterns of anterior Hox genes during Nile tilapia (Oreochromis niloticus) embryonic development. Gene Expr. Patterns 13, 104–108.

Mallatt, J., Chen, J.Y., 2003. Fossil sister group of craniates: predicted and found. J.

Morphol. 258, 1–31.
Matsuo, I., Kuratani, S., Kimura, C., Takeda, N., Aizawa, S., 1995. Mouse otx2 functions in the formation and patterning of rostral head. Genes Dev. 9, 2646–2658.
McCauley, D.W., Bronner-Fraser, M., 2003. Neural crest contributions to the lamprey head. Development 130, 2317–2327.
McCauley, D.W., Bronner-Fraser, M., 2004. Conservation and divergence of BMP2/4 genes in the lamprey: expression and phylogenetic analysis suggest a single ancestral vertebrate gene. Evol. Dev. 6, 411–422.
McGonnell, I.M., Graham, A., Richardson, J., Fish, J.L., Depew, M.J., Dee, C.T., Holland, P.W.H., Takahashi, T., 2011. Evolution of the Alx homeobox gene family: parallel retention and independent loss of the vertebrate Alx3 gene. Evol. Dev. 13, 343–351.
Medeiros, D.M., Crump, J.G., 2012. New perspectives on pharyngeal dorsoventral patterning in development and evolution of the vertebrate jaw. Dev. Biol. 371, 121–135.
Meulemans, D., Bronner-Fraser, M., 2004. Gene-regulatory interactions in neural crest evolution and development. Dev. Cell 7, 291–299.
Minoux, M., Antonarakis, G.S., Kmita, M., Duboule, D., Rijli, F.M., 2009. Rostral and caudal pharyngeal arches share a common neural crest ground pattern. Development 136, 637–645.
Minoux, M., Rijli, F.M., 2010. Molecular mechanisms of cranial neural crest cell migration and patterning in craniofacial development. Development 137, 2605–2621.
Morris, S.C., Caron, J.-B., 2014. A primitive fish from the Cambrian of North America. Nature 512, (419-U413).
Nichols, J.T., Pan, L., Moens, C.B., Kimmel, C.B., 2013. barx1 represses joints and promotes cartilage in the craniofacial skeleton. Development 140, 2765–2775.
Noden, D.M., 1978. Control of avian cephalic neural crest cytodifferentiation .1. Skeletal and connective tissues. Dev. Biol. 67, 296–312.
Northcutt, R.G., Gans, C., 1983. The genesis of neural crest and epidermal placodes – a reinterpretation of vertebrate origins. Q. Rev. Biol. 58, 1–28.
Oisi, Y., Ota, K.G., Fujimoto, S., Kuratani, S., 2013. Development of the Chondrocranium in Hagfishes, with special reference to the early evolution of vertebrates. Zool. Sci. 30, 944–961.
Parker, H.J., Bronner, M.E., Krumlauf, R., 2014. A Hox regulatory network of hindbrain segmentation is conserved to the base of vertebrates. Nature 514, 490, (+).
Parker, H.J., Bronner, M.E., Krumlauf, R., 2016. The vertebrate Hox gene regulatory network for hindbrain segmentation: Evolution and diversification Coupling of a Hox gene regulatory network to hindbrain segmentation is an ancient trait originating at the base of vertebrates. Bioessays 38, 526–538.
Pasqualetti, M., Ori, M., Nardi, I., Rijli, F.M., 2000. Ectopic Hoxa2 induction after neural crest migration results in homeosis of jaw elements in Xenopus. Development 127, 5367–5378.
Piekarski, N., Gross, J.B., Hanken, J., 2014. Evolutionary innovation and conservation in the embryonic derivation of the vertebrate skull. Nat. Commun. 5.
Renz, A.J., Gunter, H.M., Fischer, J.M.F., Qiu, H., Meyer, A., Kuraku, S., 2011. Ancestral and derived attributes of the dlx gene repertoire, cluster structure and expression patterns in an African cichlid fish. Evodevo 2.
Rose, C.S., 2014. The importance of cartilage to amphibian development and evolution. Int. J. Dev. Biol. 58, 917–927.
Ruest, L.B., Hammer, R.E., Yanagisawa, M., Clouthier, D.E., 2003. Dlx5/6-enhancer directed expression of Cre recombinase in the pharyngeal arches and brain. Genesis 37, 188–194.
Sansom, R.S., Freedman, K., Gabbott, S.E., Aldridge, R.J., Purnell, M.A., 2010. Taphonomy and affinity of an enigmatic silurian vertebrate, jamoytius kerwoodi white. Palaeontology 53, 1393–1409.
Santagati, F., Minoux, M., Ren, S.Y., Rijli, F.M., 2005. Temporal requirement of Hoxa2 in cranial neural crest skeletal morphogenesis. Development 132, 4927–4936.
Santagati, F., Rijli, F.M., 2003. Cranial neural crest and the building of the vertebrate head. Nat. Rev. Neurosci. 4, 806–818.
Sauka-Spengler, T., Meulemans, D., Jones, M., Bronner-Fraser, M., 2007. Ancient evolutionary origin of the neural crest gene regulatory network. Dev. Cell 13, 405–420.
Schultemerker, S., Hammerschmidt, M., Beuchle, D., Cho, K.W., Derobertis, E.M., Nussleinvolhard, C., 1994. Expression of zebrafish goosecoid and no tail gene-products in wild-type and mutant no tail embryos. Development 120, 843–852.
Shigetani, Y., Sugahara, F., Kawakami, Y., Murakami, Y., Hirano, S., Kuratani, S., 2002. Heterotopic shift of epithelial-mesenchymal interactions in vertebrate jaw evolution. Science 296, 1316–1319.
Shu, D.G., Luo, H.L., Morris, S.C., Zhang, X.L., Hu, S.X., Chen, L., Han, J., Zhu, M., Li, Y., Chen, L.Z., 1999. Lower Cambrian vertebrates from South China. Nature 402, 42–46.
Shu, D.G., Morris, S.C., Han, J., Zhang, Z.F., Yasui, K., Janvier, P., Chen, L., Zhang, X.L., Liu, J.N., Li, Y., Liu, H.Q., 2003. Head and backbone of the Early Cambrian vertebrate Haikouichthys. Nature 421, 526–529.
Shubin, N., Tabin, C., Carroll, S., 2009. Deep homology and the origins of evolutionary novelty. Nature 457, 818–823.
Simoes-Costa, M., Bronner, M.E., 2015. Establishing neural crest identity: a gene regulatory recipe. Development 142, 242–257.
Smith, J.J., Keinath, M.C., 2015. The sea lamprey meiotic map improves resolution of ancient vertebrate genome duplications. Genome Res. 25, 1081–1090.
Square, T., Jandzik, D., Cattell, M., Coe, A., Doherty, J., Medeiros, D.M., 2015. A gene expression map of the larval Xenopus laevis head reveals developmental changes underlying the evolution of new skeletal elements. Dev. Biol. 397, 293–304.
Square, T., Jandzik, D., Cattell, M., Hansen, A., Medeiros, D.M., 2016. Embryonic expression of *endothelins* and their receptors in lamprey and frog reveals stem vertebrate origins of complex Endothelin signaling. Sci. Rep. 6 (34282).
Stock, D.W., 2005. The Dlx gene complement of the leopard shark, Triakis semifasciata, resembles that of mammals: implications for genomic and morphological evolution of jawed vertebrates. Genetics 169, 807–817.
Stock, D.W., Ellies, D.L., Zhao, Z.Y., Ekker, M., Ruddle, F.H., Weiss, K.M., 1996. The evolution of the vertebrate Dlx gene family. Proc. Natl. Acad. Sci. USA 93, 10858–10863.
Stock, D.W., Whitt, G.S., 1992. Evidence from 18s ribosomal-RNA sequences that lampreys and hagfishes form a natural group. Science 257, 787–789.
Sugahara, F., Aota, S., Kuraku, S., Murakami, Y., Takio-Ogawa, Y., Hirano, S., Kuratani, S., 2011. Involvement of Hedgehog and FGF signalling in the lamprey telencephalon: evolution of regionalization and dorsoventral patterning of the vertebrate forebrain. Development 138, 1217–1226.
Swartz, M.E., Sheehan-Rooney, K., Dixon, M.J., Eberhart, J.K., 2011. Examination of a palatogenic gene program in zebrafish. Dev. Dyn. 240, 2204–2220.
Tahara, Y., 1988. Normal stages of development in the lamprey, lampetra-reissneri (dybowski). Zool. Sci. 5, 109–118.
Takechi, M., Adachi, N., Hirai, T., Kuratani, S., Kuraku, S., 2013. The Dlx genes as clues to vertebrate genomics and craniofacial evolution. Semin. Cell Dev. Biol. 24, 110–118.
Takio, Y., Kuraku, S., Murakami, Y., Pasqualetti, M., Rijli, F.M., Narita, Y., Kuratani, S., Kusakabe, R., 2007. Hox gene expression patterns in Lethenteron japonicum embryos – insights into the evolution of the vertebrate Hox code. Dev. Biol. 308, 606–620.
Talbot, J.C., Johnson, S.L., Kimmel, C.B., 2010. hand2 and Dlx genes specify dorsal, intermediate and ventral domains within zebrafish pharyngeal arches. Development 137, 2506–2516.
Tarazona, O.A., Slota, L.A., Lopez, D.H., Zhang, G.J., Cohn, M.J., 2016. The genetic program for cartilage development has deep homology within Bilateria. Nature 533, 86, (+).
ten Berge, D., Brouwer, A., Korving, J., Martin, J.F., Meijlink, F., 1998. Prx1 and Prx2 in skeletogenesis: roles in the craniofacial region, inner ear and limbs. Development 125, 3831–3842.
Theveneau, E., Mayor, R., 2012. Neural crest delamination and migration: from epithelium-to-mesenchyme transition to collective cell migration. Dev. Biol. 366, 34–54.
Tomsa, J.M., Langeland, J.A., 1999. Otx expression during lamprey embryogenesis provides insights into the evolution of the vertebrate head and jaw. Dev. Biol. 207, 26–37.
Wada, H., Makabe, K., 2006. Genome duplications of early vertebrates as a possible chronicle of the evolutionary history of the neural crest. Int. J. Biol. Sci. 2, 133–141.
Yanagisawa, H., Clouthier, D.E., Richardson, J.A., Charite, J., Olson, E.N., 2003. Targeted deletion of a branchial arch-specific enhancer reveals a role of dHAND in craniofacial development. Development 130, 1069–1078.
Zerucha, T., Stuhmer, T., Hatch, G., Park, B.K., Long, Q.M., Yu, G.Y., Gambarotta, A., Schultz, J.R., Rubenstein, J.L.R., Ekker, M., 2000. A highly conserved enhancer in the Dlx5/Dlx6 intergenic region is the site of cross-regulatory interactions between Dlx genes in the embryonic forebrain. J. Neurosci. 20, 709–721.
Zhang, G.J., Miyamoto, M.M., Cohn, M.J., 2006. Lamprey type II collagen and Sox9 reveal an ancient origin of the vertebrate collagenous skeleton. Proc. Natl. Acad. Sci. USA 103, 3180–3185.
Zhang, S.W., Li, J.J., Lea, R., Vleminckx, K., Amaya, E., 2014. Fezf2 promotes neuronal differentiation through localised activation of Wnt/beta-catenin signalling during forebrain development. Development 141, 4794–4805.
Zhao, Z.Y., Stock, D.W., Buchanan, A.V., Weiss, K.M., 2000. Expression of Dlx genes during the development of the murine dentition. Dev. Genes Evol. 210, 270–275.